J Solid State Electrochem (2008) 12:399–407
DOI 10.1007/s10008-007-0418-x

ORIGINAL PAPER

Pt monolayer electrocatalysts for O_2 reduction: PdCo/C substrate-induced activity in alkaline media

F. H. B. Lima · J. Zhang · M. H. Shao · K. Sasaki · M. B. Vukmirovic · E. A. Ticianelli · R. R. Adzic

Received: 5 January 2007 / Revised: 1 June 2007 / Accepted: 7 August 2007 / Published online: 18 September 2007

Abstract We measured the activity of electrocatalysts, comprising Pt monolayers deposited on PdCo/C substrates with several Pd/Co atomic ratios, in the oxygen reduction reaction in alkaline solutions. The PdCo/C substrates have a core-shell structure wherein the Pd atoms are segregated at the particle's surface. The electrochemical measurements were carried out using an ultrathin film rotating disk-ring electrode. Electrocatalytic activity for the O_2 reduction evaluated from the Tafel plots or mass activities was higher for Pt monolayers on PdCo/C compared to Pt/C for all atomic Pd/Co ratios we used. We ascribed the enhanced activity of these Pt monolayers to a lowering of the bond strength of oxygenated intermediates on Pt atoms facilitated by changes in the 5*d*-band reactivity of Pt. Density functional theory calculations also revealed a decline in the strength of PtOH adsorption due to electronic interaction between the Pt and Pd atoms. We demonstrated that very active O_2 reduction electrocatalysts can be devised containing only a monolayer Pt and a very small amount of Pd alloyed with Co in the substrate.

Keywords Electrocatalysis · Oxygen reduction · Core-shell electrocatalysts · Platinum alloys

Dedicated to Professor Oleg Petrii on the occasion of his 70th birthday on August 24, 2007.

F. H. B. Lima · E. A. Ticianelli
Instituto de Química de São Carlos, Universidade de São Paulo, CEP 13560-970, CP 780 São Carlos, São Paulo, Brazil

J. Zhang · M. H. Shao · K. Sasaki · M. B. Vukmirovic · R. R. Adzic (✉)
Department of Chemistry, Brookhaven National Laboratory, Upton, NY 11973, USA
e-mail: adzic@bnl.gov

Introduction

Considerable ongoing research is aimed at increasing the electrocatalytic activity of platinum for the oxygen reduction reaction (ORR) in both acid and alkaline media [1–8]. Some improvements were achieved, for example, in the kinetics of the ORR for Pt alloys such as Pt–V, P–Cr, Pt–Fe Pt–Co, and Pt–Ni, compared to intrinsic Pt. This enhancement was attributed to one or more of the following changes of the properties of Pt after alloying: electronegativity, Pt–Pt bond distance, number of nearest neighbors, density of states of the 5*d* band, and nature and coverage of the surface oxide layers [8–10]. Previous measurements by others of some metal alloys using X-ray absorption near edge structure (XANES) spectroscopy showed that the presence of the non-noble metal caused a decrease in the Pt 5*d* band vacancy and a shift in the *d*-band center in the oxide region [7] that they attributed to the electronic interaction of Pt with the non-noble metal, thereby reducing the reactivity of Pt for adsorbates and improving the kinetics of the ORR. The enhanced activity of the Pt atoms was ascribed to faster Pt–O^- electroreduction reflecting a lowering of the adsorption strength, and consequently, faster hydrogenation of adsorbed oxygen species.

Nørskov et al. [9–12] recently demonstrated that the catalytic reactivity of the metals can be rationalized in terms of the energy of the *d*-band center (ε_d). The Nørskov model is based on the shifting of the *d*-band center that raises or lowers the reactivity of metal catalysts. With an upshift of the *d*-band center, a distinctive anti-bonding state appears above the Fermi level. Such states are empty ones, and so bonding takes place. Accordingly, strong bonding occurs if anti-bonding states are upshifted though the Fermi level (and become empty), while the opposite occurs if they are shifted down through the Fermi level (and become filled).

For Pt monolayer catalysts, the position of the ε_d depends both on the strain (geometric effects) and on the electronic interaction between the platinum monolayer and its substrate (ligand effect) [11]. Other research groups and ours demonstrated [13, 14] that metal monolayer on different metal substrates is subject to a tensile or compressive force the strength of which is determined by the substrate's lattice parameter. This force entails a variation in the width of the *d*-band, thereby shifting its center to preserve the degree of *d*-band filling.

In an earlier work [15], we described the effects of the substrate on the activity of the ORR in an acid electrolyte on Pt monolayers deposited on the surfaces of different single-crystal metal substrates. On Au (111), the Pt atoms experience tensile force, thereby narrowing the Pt *d*-band, with an upshift in the *d*-band center, leading to stronger $Pt–O^-$ adsorption. On the other hand, on Ir (111), the Pt atoms are under compressive strain that downshifts the *d*-band center, and consequently, weakens $Pt–O^-$ adsorption. Expressing the kinetic currents, obtained from the Koutecky–Levich plots for O_2 reduction on the platinum monolayers on various substrates at 0.8 V, as a function of the calculated ε_d of the Pt monolayers generates a volcano-like curve, with Pt/Pd(111) showing the maximum activity. To interpret the experimental findings on the ORR activity of the platinum monolayers, additional density functional theory (DFT) calculations were undertaken to derive details of the thermochemistry and kinetics of two representative elementary reaction steps: O–O bond breaking, and O–H bond formation. That is, to understand why the highest activity is achieved by certain surfaces with a combination of properties allowing adsorption of oxygen strong enough for the O–O bond breaking while permitting a facile electroreduction of $Pt–O^-$. From the experimental results and the theoretical calculations, we associated the superior ORR catalytic activity of Pt/Pd(111) with those properties in addition to its having reduced OH coverage.

Such variations of the Pt *d*-band center, or variations of Pt reactivity, also were demonstrated for alloys of Pt that form a Pt "skin" catalyst due to the surface segregation of Pt on another metal. Alloying Pt with Co [14], where Co the host element and Pt atoms the segregated solute, downshifts the *d*-band center of Pt atoms. The observed change is due to an electronic effect resulting from a strong Pt–Co interaction and from the mismatch of their lattices that promotes a Pt–Pt compressive strain. For O_2 reduction in acid media, the lowering of Pt *d*-band center in Pt–Co was shown to lead to weaker $Pt–O^-$ adsorption, so facilitating faster $Pt–O^-$ hydrogenation, and thus, increasing O_2 reduction kinetics, in accordance with a previous report by Lima et al. [3].

The objective of the present contribution was to evaluate the electrocatalytic activity of Pt monolayers deposited on different dispersed substrates for the O_2 reduction in alkaline media. The substrates were carbon-dispersed PdCo core-shell nanoparticles (PdCo/C) with different atomic ratios, wherein the Pd atoms are segregated to the surface. Platinum was deposited in a monolayer amount on the surface of the core-shell nanoparticles by the galvanic displacement by Pt of a Cu monolayer laid down by underpotential deposition (UPD) [1]. Using non-noble metals as a core facilitates a reduction of the noble metal's content, while maintaining the full activity of a Pt monolayer by ensuring properly tailored electronic and/or geometric effects. The choice of the metals constituting the shell and core was based on considering the segregation properties of the two metals, and their electronic- and strain-inducing effects on the Pt monolayer.

Experimental

The carbon-supported PdCo/C core-shell nanoparticles were formed by Pd surface segregation from Pd/Co mixtures with atomic ratios of 1:0, 2:1, 1:5, and 1:10, all 20 wt% on carbon (Vulcan X-72C). Their synthesis involved impregnating the carbon nanoparticles with mixed solution of the noble metal and non-noble-metal salts. Pd was obtained from $PdCl_3$, Pt from K_2PtCl_4, and Co from $CoCl_2$ (supplied by Alfa Aesar). Almost-dry slurry of carbon and the metal salts was reduced using H_2 gas at 500 °C. To segregate the noble metal at the surface, the mixtures were exposed to 850 °C under a H_2 atmosphere for 1 h. Pd/C and Pt/C (20 wt%) were purchased from E-TEK-T; in some cases, Pd/C was thermally treated as above (850 °C in a H_2 atmosphere). The Pt monolayer on the as-received Pd/C substrate is designated as Pt/Pd/C, while the thermally treated substrate is designated as Pt/Pd/C (850 °C).

The Pt monolayer was prepared by the galvanic displacement by Pt of an underpotentially deposited (UPD) Cu monolayer [1]. After depositing Cu from 50 mMol/l $CuSO_4$ and 0.10 Mol/l H_2SO_4 solutions, the electrodes were rinsed to remove Cu^{2+} from the solution film and immersed in a 1.0 mMol/l K_2PtCl_4 in 50 mMol/l H_2SO_4 solution in an Ar atmosphere. Allowing 2 min for Pt to completely replace Cu, the electrodes then were removed from the solution and rinsed again. All these operations were carried out in a multi-compartment cell in an Ar atmosphere to prevent the oxidation of Cu adatoms in contact with oxygen in air. The deposition of a Pt monolayer on the surfaces of different substrates was verified by cyclic voltammetry.

The working electrodes were prepared by dispersing the catalysts as an ultrathin layer over a glassy carbon rotating disk, 5-mm diameter (0.196 cm^2), or rotating ring-disk

electrode (Pine Instruments, Grove City, PA, USA). The layers were prepared, starting with an aqueous suspension of 2.0 mg/ml of the metal/C produced by its ultrasonical dispersion in pure water (Millipore) [13]. A 10-μl aliquot of the suspension was pipetted on to the top of the glassy carbon substrate's surface. After the water had evaporated under a low vacuum, 10 μl of a diluted Nafion solution (from 5%, Aldrich) was pipetted on to electrode surface catalyst to attach the catalytic particles on the glassy carbon electrode substrate, and then it was dried. The mass contents of noble metals in the thin layer were as follows: Pd in Pd/C 23.8 μg/cm^2, Pd in Pd_2Co 18.5 μg/cm^2, Pd in $PdCo_5$ 6.1 μg/cm^2, and Pd in $PdCo_{10}$ 3.57 μg/cm^2.

Ag/AgCl/KCl 3 mol/l leak-free electrodes (Cypress Lawrence, KS, USA) were used as a reference, while all potentials, *E*, are quoted with respect to the reversible hydrogen electrode. All measurements of the ORR were made in a 0.1 mol/l NaOH electrolyte, prepared from high purity reagents (Merck) and water, purified in a Milli-Q (Millipore) system. Polarization curves were recorded using a linear sweep at 5 mV/s in the cathodic direction in the potentiostatic mode as a function of rotation rate.

Results and discussion

Figure 1a and b shows the voltammetry responses obtained for the UPD of Cu on Pd_2Co/C and $PtCo_5$/C nanoparticles (solid line) and the corresponding voltammetry curves for Pd_2Co/C and $PtCo_{10}$/C in solutions lacking Cu ions. The charge associated with the UPD of Cu on Pd/C was of 5.8 mC/cm^{-2}, while for all PdCo/C nanoparticles, it was close to 2.0 mC/cm^2, in good agreement with the real surface area estimated from the particles' sizes [16]. The several peaks positive to the onset of Cu bulk deposition are likely to be associated with the Cu UPD on different Pd crystallographic faces.

Figure 2a and b shows the voltammograms for the Pt monolayer deposited on Pd/C, before and after thermal treatment at 850 °C in H_2 atmosphere, while Fig. 3 has the results for Pt monolayers on PdCo/C nanoparticles of different atomic ratios. They depict the characteristic hydrogen adsorption/desorption and oxide-formation regions of Pt in alkaline media, evidencing a high degree of coverage of the Pt adatoms. Figure 2 reveals a considerable decrease in the magnitude of the voltammetric currents after thermal treatment of the Pd/C particles; it suggests that the particles' size has increased, causing a decrease of the surface area. Figure 3 indicates that this effect, caused by heating, declines with an increase in the Co/Pd ratio. The latter may be due to alloying with Co atoms, so stabilizing the particle's size due to the stronger Pd–Co bond compared to that of Pd–Pd.

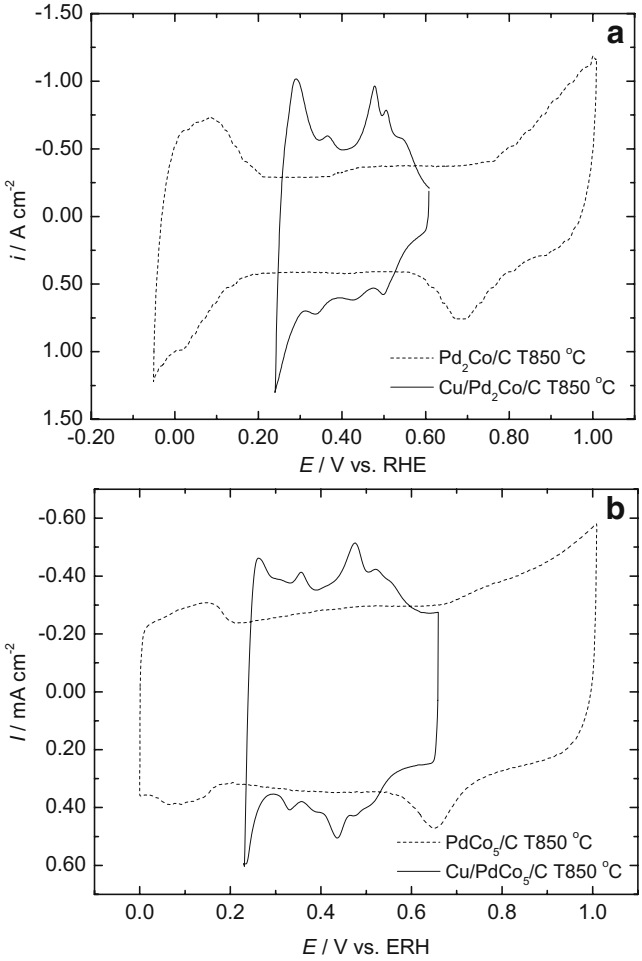

Fig. 1 Voltammetry curves for the underpotential deposition of Cu on carbon-supported Pd_2Co (**a**) and $PdCo_5$ (**b**) nanoparticles on a glassy carbon disk (*solid line*) in 0.05 M H_2SO_4 with 50 mM Cu^{2+} and the curves for the same surfaces in the absence of Cu (*dashed line*); sweep rate 50 and 20 mV/s, respectively

As we discussed previously [14], the noble-metal shell in the core-shell nanoparticle has two actions: one is that it protects the non-noble core from contacting the electrolyte, thus, preventing its dissolution, and second, it improves the catalytic properties of the Pt monolayer. This latter can be a consequence of changing the monolayer's electronic properties due to a ligand effect and/or by inducing a strain in it. Thus, the characteristics of the surface segregation of the noble metal on the substrates is an important aspect of this research particularly because it modulates the stability of systems containing high quantities of non-noble metals. For the host–solute systems investigated here, the presence of a surface-segregated Pd layer is corroborated by the findings from DFT calculations [9]. The surface segregation of Pd and the protection of the Co core from dissolving are apparent from two sets of results. One is from voltammetry of the PdCo materials that revealed no anodic currents due to the oxidation/dissolution of Co. The other comes from

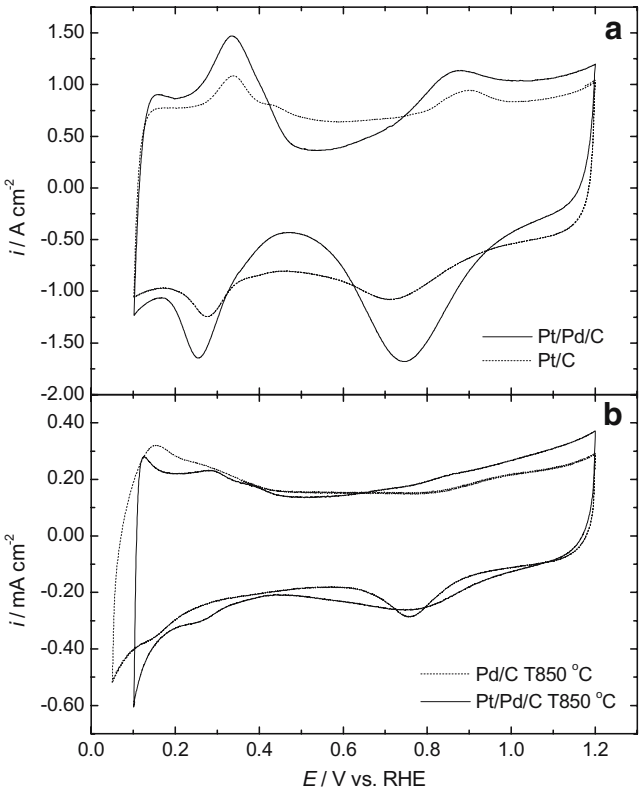

Fig. 2 **a** Voltammetry curves for a Pt monolayer, obtained by galvanic displacement of a Cu monolayer, on as-received Pd/C nanoparticles compared to that obtained for Pt/C; **b** voltammetry curves for a Pt monolayer obtained by galvanic displacement of the Cu monolayer on the Pd/C T850 °C compared to that obtained for the pure Pd/C T850 °C. The electrolyte solution is 0.1 mol/L NaOH and the sweep rate 50 mV/s

the voltammetry responses of a P/PdCo/C surface showing the UPD of H, indicating that the surface mainly consists of Pt. The high-resolution transmission electron microscopy (TEM) image of a Pd/Co/C nanoparticle (Fig. 4) verifies

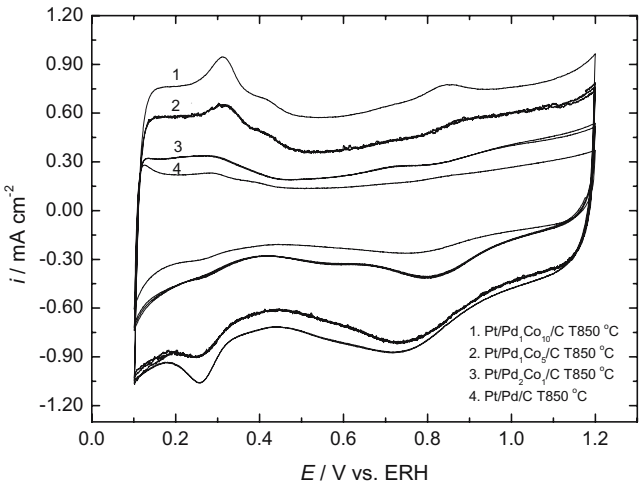

Fig. 3 Voltammetry curves for a Pt monolayer, obtained by galvanic displacement of the Cu monolayer, on the PdCo/C T850 °C substrates at different atomic ratios in 0.1 mol/l NaOH; sweep rate 50 mV/s

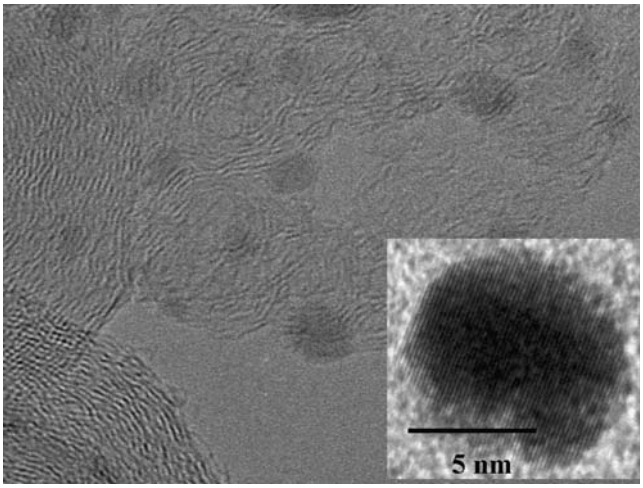

Fig. 4 Low- and high-resolution TEM images of Pd/Co/C nanoparticles. The different interference fringes of the layers close to the surface compared to the bulk point to the presence of a Pd shell around a Co core

this interpretation wherein the different interference fringes of the layers close to the surface compared to the bulk point to the presence of a shell around a core.

Figure 5 plots the polarization curves for the ORR at the disk electrode and the currents for HO_2^- oxidation at the ring electrode obtained at several rotation speeds for the Pt/Pd/C catalyst. The reaction is diffusion-controlled at potentials below 0.7 V and is under mixed, diffusion-kinetic control between 0.7 and 0.95 V. The linear dependence of the limiting diffusion current on the square

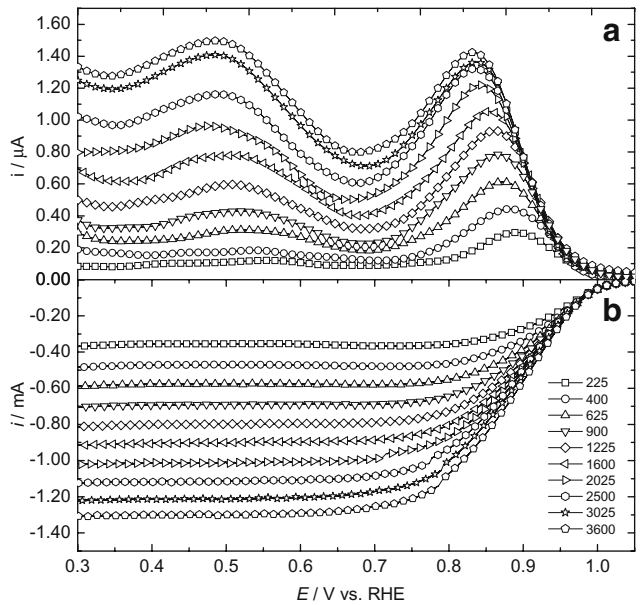

Fig. 5 Polarization curves obtained with a rotating disk-ring electrode for O_2 reduction on a Pt monolayer on Pd/C substrate in 0.1 mol/l NaOH solution. **a** Ring currents; **b** disk currents. Rotation rates are indicated in the graph; sweep rate 5 mV/s; ring potential 1.2 V; ring and disk areas are 0.037 and 0.1636 cm^2, respectively; collection efficiency N=0.21

root of the rotation rate was verified for these data [17]. The ring response (Fig. 5a) indicates the formation of very small amounts of HO_2^-, the intermediate of the ORR.

Figure 6 displays the polarization curves at 1,600 rpm for the ORR on the Pt monolayers deposited on the as-received and thermally treated (850 °C) commercial Pd/C substrates. It also includes the findings from Pd/C and on Pt/C commercial substrates. The half-wave potential for the ORR for the Pt/Pd/C substrate is higher than that for Pt/Pd/C (850 °C). The lower half-wave potentials, i.e., the activity, observed for the heat-treated materials can be attributed to a decrease in their surface area, inferred from the voltammetry curves in Fig. 2.

Figure 7 gives the polarization curves for O_2 reduction on the Pt monolayer deposited on the PdCo/C substrates and on the substrates consisting of different Pd/Co atomic ratios. Although their half-wave potentials are below those of Pt/Pd/C due to their lower surface area (higher particle size), an important and surprising fact is that the half-wave potentials for O_2 reduction remain essentially constant for different Pd/Co atomic ratios. This correspondence may reflect surface enrichment by Pd due to the surface segregation of Pd atoms in the substrate particles [9]. The limiting current densities for all electrocatalysts are close to that of Pt/C. As shown before [17, 18], the ORR in alkaline media on this catalyst follows a parallel pathway [19]. Despite this particularity, the results in Figs. 6 and 7 indicate that the behavior of the ORR is very similar on Pt/C and the Pt monolayer catalysts on the several substrates we investigated.

Further analysis of the disk-ring measurements was carried out in terms of the Koutecky–Levich plots and of the *J-S* plots (intercepts vs slopes from the $N{\cdot}I_D/I_R$ vs $\omega^{-1/2}$ plots) [20]. The linearity and parallelism of the Koutecky–Levich plots (not shown) indicates a first-order reaction for

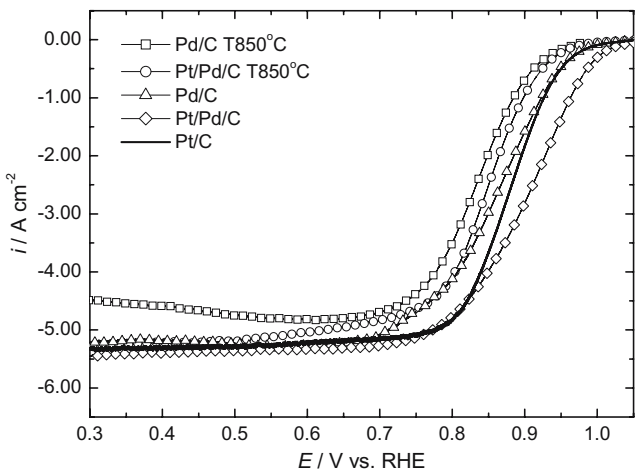

Fig. 6 Comparison of polarization curves for O_2 reduction on Pt monolayer deposited on Pd/C and on Pd/C T850 °C and on the pure substrates. The electrode geometric area is 0.163 cm^2

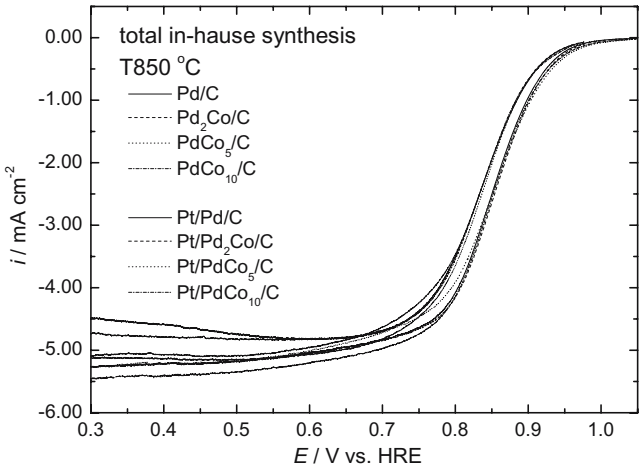

Fig. 7 Comparison of polarization curves for O_2 reduction on Pt monolayer deposited on the PdCo/C T850 °C with different atomic ratios and on the pure substrates. The electrode geometric area is 0.163 cm^2

molecular oxygen. Although the analysis of the *J-S* plots indicate a parallel mechanism of the ORR, dividing I_D with the negligible ring currents yielded much scatter in the plots, rendering them unreliable. The percentage of O_2 molecules forming HO_2^- in a two-electron reduction on a Pt monolayer on Pd/C catalyst in 0.1 M NaOH as a function of the potential was calculated from the ring currents [14] and is given in Table 1.

We compared the ORR electrocatalytic activities of the Pt monolayers using mass-transport corrected Tafel plots obtained from the currents normalized by the mass of platinum (Fig. 8) and the total amount of noble metals (Fig. 9) in the catalyst layer. The linearity of the plots is poor. However, a linear region with the Tafel slope of −60 mV/dec can be traced at low current densities. The curves change slopes at high currents, and apparently, a slope of −120 mV/dec begins to appear [17]. This can be explained in terms of the coverage of adsorbed oxygen, which follows a Temkin isotherm (high coverage) at low overpotentials and a Langmuir isotherm (low coverage) at high overpotentials. We observed from the results in Figs. 8 and 9 that the Pt/Pd/C electrocatalyst departs from the −60 mV/dec region at lower overpotentials than the others, suggesting that the

Table 1 Percentage of O_2 molecules forming HO_2^- in a two-electron reduction on a Pt monolayer on Pd/C catalyst in 0.1 M NaOH

Pt/Pd/C (V)	$X_{HO_2^-}$ /(%)
0.9	1.40
0.8	0.87
0.7	0.22
0.6	0.64
0.5	0.96
0.4	0.64

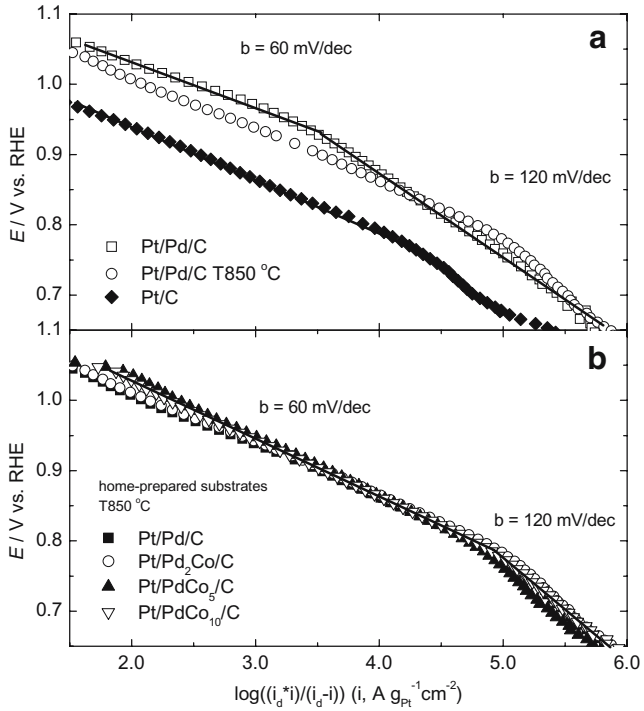

Fig. 8 Mass-transport corrected Tafel plots for the ORR on **a** Pt monolayer deposited on Pd/C and on Pd/C T850 °C, **b** Pt monolayer deposited on the PdCo/C T850 °C at different atomic ratios in NaOH 0.1 mol/l at 25 °C. ω=1,600 rpm. Currents normalized by the mass of Pt in the catalyst layer

electroreduction of Pt-adsorbed oxygenated intermediates (PtOx) takes place at lower overpotentials in this catalyst than for other materials. For Pt monolayers on thermally treated Pd/C and on $PdCo_x$/C, higher Tafel slopes are observed at lower currents compared to Pt/C, which increase with decreasing atomic ratio of Pd/Co. Accordingly, the electroreduction of PtOx on the Pt monolayer deposited on the PdCo/C materials may be more facile compared to that on Pt/C. In other words, the Pt–oxygen bonding to the Pt monolayers on Pd-based materials probably is weaker than it is to Pt/C.

The size of the particles in different substrates apparently plays a role in determining the potentials of the transition from the −60 to the −120 mV/dec slopes for Pt/Pd/C, Pt/Pd/C (850 °C) and Pt/PdCo/C catalysts as is inferred from the voltammetry curves in Fig. 2. It seems that the smaller substrate particles exert more pronounced electronic effect on the Pt monolayers than do the larger ones, so explaining the early change in the Tafel slope for the Pt/Pd/C catalyst and its increasing trend at low currents with decreasing of the Pd/Co atomic ratio (lower particle size). For the same Pt loading (Fig. 8), Pt/Pd/C and Pt–Pd/C (850 °C) display higher activity than does Pt/C (Fig. 8a), while approximately the same activity is achieved for the Pt monolayers deposited on several different PdCo/C substrates (Fig. 8b). These observations are consistent to the results in Fig. 7 that shows the closeness of the values of the half-wave potentials for Pt on PdCo/C catalysts, including $Pt/PdCo_{10}$/C. As discussed above, this finding indicates that these surfaces are covered by surface-segregated Pd atoms with similar properties. Thus, for a constant total noble metal (Pt + Pd) loading (Fig. 9), the results point to high activity for Pt/Pd/C, followed by Pt/C, and Pt/Pd/C (850 °C; Fig. 9a). Comparing the Tafel plots for the Pt monolayers on different PdCo/C substrates (Fig. 9b) reveals a high activity for $Pt/PdCo_{10}$/C resulting from its low noble-metal content, which is replaced by Co. In bar plots of the Pt mass activity (Fig. 10a) for five different Pt monolayer electrocatalysts compared with the commercial Pt sample, the former have a fivefold larger activity. However, comparing the total noble-metal-content mass activities reveals somewhat higher activity in the commercial Pt/C samples (Fig. 10b). As the price of Pd is one fourth that of Pt, these catalysts may still be attractive for practical applications.

DFT calculations indicate a small increase of the activity of a pseudomorphic monolayer of Pt on a Pd single crystal compared with pure Pt due to a smaller PtOH coverage and/or faster O–H bond formation as a consequence of the shift of the *d*-band center [1, 15]. Our data indicate that the high activity of Pt monolayers deposited on various substrates are a consequence of changes in the *d*-band properties of

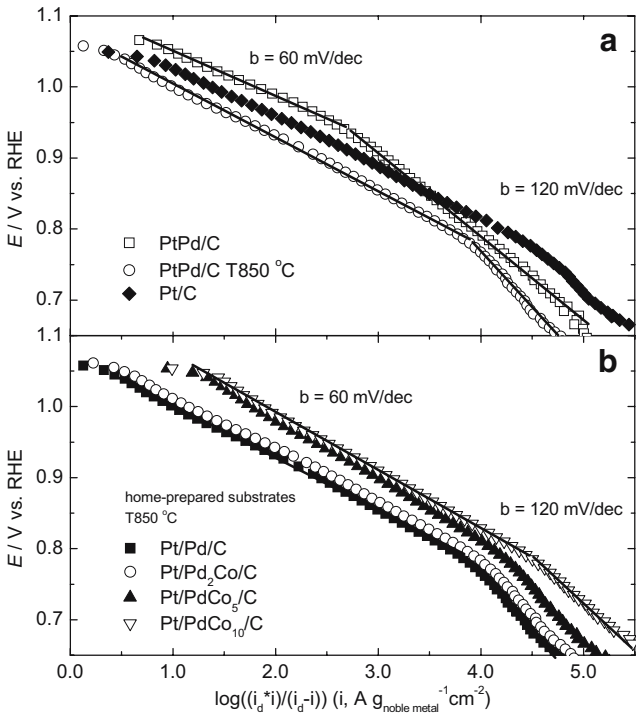

Fig. 9 Mass-transport corrected Tafel plots for the ORR on **a** Pt monolayer deposited on Pd/C and on Pd/C T850 °C, **b** Pt monolayer deposited on the PdCo/C T850 °C at different atomic ratios in NaOH 0.1 mol/l at 25 °C. ω=1,600 rpm. Currents normalized by the mass of noble metal in the catalyst layer

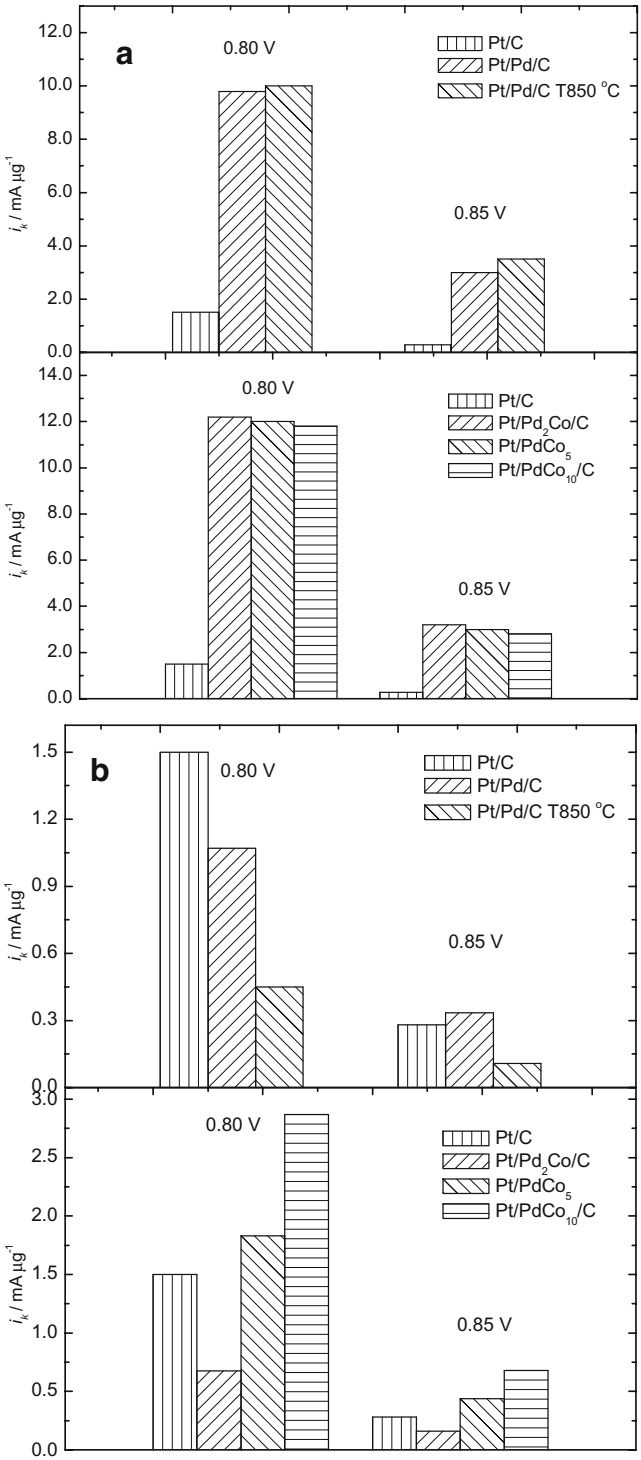

Fig. 10 Bar plots of the Pt-mass activity for five different Pt monolayer electrocatalysts compared with the commercial Pt sample (**a**) and the total noble-metal-content mass activity (**b**) at 0.85 and 0.8 V obtained from Figs. 8 and 9

the Pt monolayers caused by lattice mismatch and the strong electronic interaction of the Pt atoms with the substrates. Any possible mismatch between the lattice constants for the Pt monolayer on Pd/C or on the PdCo/C nanoparticles would be small, caused mostly by the contraction of Pd on the core comprising mainly Co atoms. The contraction of the Pd lattice and the electronic interaction with the Co atoms would enhance the activity of Pd for the O_2 reduction, as we demonstrated recently [21]. Consequently, a compressed Pd substrate can generate only a small compressive strain in a Pt monolayer, and, probably, a comparably small decrease in its reactivity. The effect of *d*-band filling of the substrate also is expected to be limited, as the fractional filling of the *d*-bands of Pd and Pt is the same. However, their interaction can be anticipated to engender some charge redistribution through hybridization of the states from each atom. So, the increased catalytic activity observed for the Pt monolayers on PdCo/C substrates may be ascribed to modification of the Pt 5*d* electronic properties caused mainly by the electronic interaction with Pd or by Pd electronically modified by the Co atoms. The decrease of PtOH coverage can be attributed to an electronic (ligand) effect of the Pd/C or PdCo/C substrate, which can account for the greater activity of the Pt/PdCo/C electrocatalysts.

For Pd-M alloys, Fernandez et al. [22] and Wang and Balbuena [23] proposed thermodynamic guidelines for designing non-Pt electrocatalysts for the ORR. Fernandez et al. theorized that the metal, M, affords the sites for breaking the O–O bonds of oxygen. The O atoms then can migrate to Pd sites to be reduced to water at a relatively high potential. For Pd with fully occupied valence d-orbitals, Wang and Balbuena [23] believed that alloying with Co with unoccupied valence d-orbitals significantly lowers the Gibbs free energy both for the first charge-transfer step and for the step involving the reduction of intermediates (O/OH). However, these thermodynamic models did not account for strong surface segregation in the Pd–Co system. This brief overview

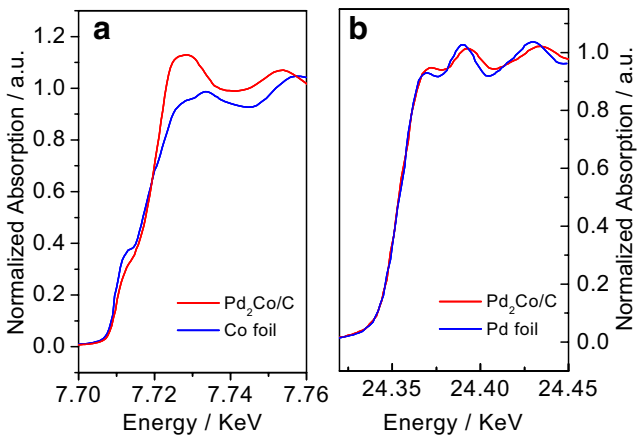

Fig. 11 Comparison of XANES data of Pd_2Co/C with Co and Pd foils at 0.57 V (double layer region). Co K edge for Pd_2Co/C and pure Co foil (**a**) and Pd K edge for Pd_2Co/C and pure Pd foil (**b**)

indicates that most proposed models for enhanced catalytic activity converge, or are not incompatible with the central role of the *d*-band center [10].

We gathered additional information on the Pd_2Co/C alloy by in situ XANES technique for both its Co and Pd constituents. Figure 11a, and b plots the spectra obtained at 0.57 V, i.e., in the double-layer region of Pd. The significant changes of the K-edge spectra for both Co and Pd of Pd_2Co/C compared with the corresponding metal foils indicate a strong interaction between Pd and Co. For the Co K edge, the intensity of pre-edge peak falls, while the white line increases dramatically compared with the Co foil. The changes in intensity of these peaks suggest that the occupancy of d orbitals of Co has decreased. For the Pd K edge, the intensity of white line is a little higher than that from the Pd foil, indicating an increase in the vacancies of the 4*d*-band compared with pure Pd. Pd is a relatively reactive metal; thus, its position is on the ascending branch of the volcano plot for the ORR, just below Pt [24]. Therefore, to enhance the catalytic property of Pd-based catalysts, the ε_d of Pd should shift to a lower energy position. From our XANES results, a downshift of its ε_d was expected to result from the larger vacancy of 4*d*-band in the Pd–Co alloy and the increased kinetics of the ORR. This downshift is caused by the ligand effect of Co atoms on Pd. After high-temperature annealing, the palladium atoms diffuse to the surface of the alloy nanoparticles, as palladium and cobalt represent a strongly segregated system [25]. Thus, a Pd-rich 'skin' should be formed on the Pd_2Co nanoparticle. From a cyclic voltammogram, we detected no individual peak of cobalt, seemingly indicating that it was fully incorporated into palladium forming an alloy, while a Pd-rich 'skin' was formed on the alloy's surface. Such Pd skin acts as a suitable substrate for a Pt monolayer, so improving its activity for the ORR.

The idea that a Pd skin is formed also is supported by the unsymmetrical X-ray diffraction line of the Pd_2Co alloy [21]. A compressive strain apparently exists on the surface of Pd–Co alloy based on the fact that the Pd interatomic distance in Pd_2Co bulk alloy is significantly smaller than that of pure Pd particle (0.272 vs 0.275 nm), with a mismatch of about 1.1%. The compressive strain is known to shift the ε_d to a position of lower energy, as mentioned above. Thus, the combination of the compressive strain and ligand effects reduces the adsorption energy of adsorbates by lowering the ε_d of the Pd skin. Consequently, the ORR kinetics of the Pd–Co catalyst are enhanced.

Conclusions

We demonstrated that the Pt monolayers deposited on PdCo/C and on PdCo/C core-shell substrate nanoparticles have high activity in the O_2 reduction reaction. Any possible mismatch between the lattice constants of the Pt monolayer and the Pd phase on Pd/C or PdCo/C substrate should be small. Consequently, only a small compressive strain in a Pt monolayer is e induced; thus, only a comparably small decrease in its reactivity is expected. Therefore, the increased activity for the O_2 reduction on Pt monolayer on the Pd/C or PdCo/C substrate can be ascribed to a decline in PtOH adsorption strength due to electronic interactions between the Pt and Pd atoms as indicated by DFT theoretical calculations.

We showed that it is possible to devise the ORR electrocatalysts containing only a fractional amount of Pt and a very small amount of Pd in the substrate whose activity is higher than that of the state-of-the-art carbon-supported Pt electrocatalysts. This enhancement is achieved by the surface segregation of the substrate noble metal, thereby facilitating their much better utilization. Consequently, the costs of the oxygen cathodes in these electrocatalysts could be considerably reduced.

Acknowledgments This work is supported by US Department of Energy, Divisions of Chemical and Material Sciences, under the Contract No. DE-AC02-98CH10886. F.H.B.L. acknowledges support from CAPES and FAPESP, Brazil.

References

1. Zhang J, Mo Y, Vukmirovic MB, Klie R, Sasaki K, Adzic RR (2004) J Phys Chem B 108:10955
2. Paulus UA, Wokaun A, Scherer GG, Schmidt TJ, Stamenkovic V, Radmilovic V, Markovic NM, Ross PN (2002) J Phys Chem B 106:4181
3. Lima FHB, Giz MJ, Ticianelli EA (2005) J Braz Chem Soc 16:328
4. Min MK, Cho JH, Cho KW, Kim H (2000) Electrochim Acta 45:4211
5. McBreen J, Mukerjee S (1995) J Electrochem Soc 142:3399
6. Mukerjee S, Srinivasan S, Soriaga MP, McBreen J (1995) J Electrochem Soc 142:1409
7. Arico AS, Shukla AK, Kim H, Park S, Min M, Antonucci V (2001) Appl Surf Sci 172:33
8. Shukla AK, Neergat M, Bera P, Jayaram V, Hegde MS (2001) J Electroanal Chem 504:111
9. Hammer B, Norskov JK (1995) Surf Sci 343:211
10. Hammer B, Norskov JK (2000) Advances in catalysis, vol 45. Academic, San Diego, p 71
11. Kitchin JR, Norskov JK, Barteau MA, Chen JG (2004) J Chem Phys 120:10240
12. Greeley J, Norskov JK, Mavrikakis M (2002) Annu Rev Phys Chem 53:319
13. Schmidt TJ, Gasteiger HA, Stab GD, Urban PM, Kolb DM, Behm RJ (1998) J Electrochem Soc 145:2354
14. Zhang J, Lima FHB, Shao MH, Sasaki K, Wang JX, Hanson J, Adzic RR (2005) J Phys Chem B 109:22701
15. Zhang JL, Vukmirovic MB, Xu Y, Mavrikakis M, Adzic RR (2005) Angew Chem Int Edit 44:2132

16. Benfield RE (1992) J Chem Soc Faraday Trans 88:1107
17. Perez J, Gonzalez ER, Ticianelli EA (1998) Electrochim Acta 44:1329
18. Lima FHB, Ticianelli EA (2004) Electrochim Acta 49:4091
19. Adzic RR (1998) In: Lipkowski J, Ross PN (eds) Electrocatalysis. Wiley, New York, pp 197–242
20. Anastasijevic NA, Vesovic V, Adzic RR (1987) J Electroanal Chem 229:305 and 317
21. Shao MH, Huang T, Liu P, Zhang J, Sasaki K, Vukmirovic MB, Adzic RR (2006) Langmuir 22:10409
22. Fernandez JL, Walsh DA, Bard AJ (2005) J Am Chem Soc 127:357
23. Wang YX, Balbuena PB (2005) J Phys Chem B 109:18902
24. Norskov JK, Rossmeisl J, Logadottir A, Lindqvist L, Kitchin JR, Bligaard T, Jonsson H (2004) J Phys Chem B 108:17886
25. Ruban AV, Skriver HL, Norskov JK (1999) Phys Rev B 59:15990